Lowland Technology International 2018; 20 (3): 313-320
International Association of Lowland Technology (IALT): ISSN 1344-9656

Research Paper

Simulation and prediction of wetland vegetation type based on CA-Markov model

D.J. Guan [1], S.J. Qu [2], S.S. Yang [3] and Y.X. Zeng [4]

ARTICLE INFORMATION

Article history:

Received: 06 November, 2017
Received in revised form: 21 March, 2018
Accepted: 25 August, 2018
Publish on: 07 December, 2018

Keywords:

Wetland
Vegetation type
Simulation and prediction
Three Gorges Reservoir

ABSTRACT

The construction of The Three Gorges Reservoir has changed wetland vegetation type and reconstituted Hydro-fluctuation belt pattern. In this paper, we use the improved method to extract the Hydro-fluctuation belt with clear boundary and four types of wetland land use types, and analyze the dynamic changes of wetland land use types through the area change and structural change. The CA-Markov model is used to simulate the distribution map of the wetland utilization type in the next 20 years. The results show that the vegetation coverage stability of the fluctuate belt has improved; the activity of each type is reduced and the stability is enhanced; the transfer of the terrestrial plants is affected by the bare soil, and the water body has a great influence on the centroid transfer of the hygrophyte; it can be seen from the prediction of the distribution pattern of the future Hydro-fluctuation belt that the stability of the Hydro-fluctuation belt will gradually decrease if the environment of the Hydro-fluctuation belt is not protected by human intervention.

1. Introduction

As an important ecological protection area in the waters of the Yangtze River, the Hydro-Fluctuation Belt of Three Gorges Reservoir Area has self-evident ecological value. As the core zone of the Hydro-Fluctuation Belt, the Fuling district has undergone dramatic changes. In addition, with the rapid development of a market economy as well as the vigorous advancement of the urbanization process, vegetation type of the Fuling Hydro-Fluctuation Belt in the Three Gorges Reservoir Area has been impacted by human activity. How to reasonably use Hydro-Fluctuation Belt resources, how to adjust the relationships between different vegetation types of Hydro-Fluctuation Belt, how to understand current wetland use conditions and how to determine future wetland development have become urgent problems requiring in-depth study.

At present, the fluctuation belt is generally considered as the intermediate transition zone formed by the repeated fluctuation of reservoir water level. And to study the environment of the Hydro-fluctuation belt needs a more accurate extraction method in water body range. There are currently numerous water information extraction methods. For example, Ma and Wan apply the transformed degradation results of rock to rock mass to calculate the stability and failure mode changes of landslide over time, and to guide engineering through

[1] Professor, College of Architecture and Urban Planning, Chongqing Jiaotong University, Chongqing 400074, CHINA, guandongjie_2000@163.com
[2] Graduate student, College of Architecture and Urban Planning, Chongqing Jiaotong University, Chongqing 400074, CHINA,569350442@qq.com
[3] Graduate student, College of Architecture and Urban Planning, Chongqing Jiaotong University, Chongqing 400074, CHINA, 240197442@qq.com
[4] Graduate student, College of Architecture and Urban Planning, Chongqing Jiaotong University, Chongqing 400074, CHINA,992701681@qq.com
Note: Discussion on this paper is open until June 2019

experiment based on hydro-fluctuation belt water-rock interaction of Three Gorges Reservoir area (Ma et al. 2016; Wan et al. 2017). Liu et al. examined use of white mulberry in the China's Sloping Land Conversion Program to protect water quality and conserve soil in the Three Gorges Reservoir (Liu et al. 2016). Li et al. assessed the vegetation risk of different risk areas and various vegetations respectively based on improved relative risk assessment model (RRM) taking Xiangxi river Hydro-fluctuation belt as an example (Li et al. 2016). Jiang et al. analyzed the soil stability of mulberry forestlands at different water levels in the hydro-fluctuation belt by analyzing and comparing the changes between soil physical and mechanical properties (Jiang et al. 2015). Of all the research models, the dimidiate pixel model is the simplest and the most widely used mixed pixel decomposition method (Zhang et al. 2017). Nevertheless, the model ignores the complexity of land surface, additionally, it will cause great uncertainty through selecting the extreme point to estimate the result.

At present, vegetation coverage change in the Hydro-Fluctuation Belt is an important factor that affects the ecological environment and has become a central issue in land use change and sustainable development research (Liu and Willison, 2013). Vegetation coverage change is a very complex dynamic process driven by natural and human factors with a very complex mechanism. Vegetation coverage change simulation is among the main approaches for improving the driving mechanisms of wetland, supporting urban planning and policy formulation and evaluating the effects of land use on the ecological environment. For example, Guan et al. dynamically simulated future spatiotemporal land use changes in the Japanese city of Saga by introducing the natural and socioeconomic factors affecting land use into the cellular automata (CA)–Markov model (Guan et al., 2011); Lin et al. characterized the spatiotemporal dynamics of the wetland landscape in the Zhoushan Islands during 1985-2015 to reveal the spatially explicit influential indicators (Lin et al., 2018); Liu et al. developed a new conditional random field model to integrate multi-view information and context information for improving land cover classification accuracy (Liu et al., 2018). Li et al. employed the self-organizing map neural network method to identify the land cover changes in Inner Mongolia and characterize the dynamic change map by using the grid cell method (Li et al., 2018). Mariana et al. combined logistic regression, Markov chain methods and a multi-objective land allocation model into a hybrid geo simulation model to simulate the spatiotemporal trends of change in open wetlands (Mariana et al., 2019).

Despite the rich discussion of wetland models, the following two essential aspects have been less commonly studied over the long term: (1) extraction and estimation of vegetation coverage in the Hydro-fluctuation belt are especially lacking; (2) spatio-temporal simulation of vegetation coverage in the Hydro-fluctuation belt is especially lacking.

As the world's largest artificial riparian zone, the ecological problem research of Three Gorges Reservoir area is a preliminary study, currently mainly focusing on ecological restoration of riparian belt, vegetation succession, ecological system changes of riparian belt, restoration and reconstruction of wetland vegetation, distribution management and development dynamic simulation of riparian belt and so on. (Gao et al. 2011; Huang et al. 2013; Nie et al. 2017).

Against this background, our objective is to extraction and simulate of vegetation coverage type in the Hydro-fluctuation belt. In this paper, we explore the spatial and temporal evolution characteristics of vegetation coverage through research the change of area and structure of wetland utilization types in the reservoir area. Markov model was used to predict area change of wetland vegetation type. CA model was used to simulate the distribution patterns of wetland utilization patterns in 2018, 2023, 2028 and 2033. The results are anticipated to provide theoretical and evidenced support for the Three Gorges Reservoir Environmental decision.

2. Study area and data processing

2.1 Study area

The Fuling district of the Three Gorges reservoir is at the hinterland of the Three Gorges reservoir in the Middle East of Chongqing city (**Figure 1**). The study area lies between latitude 29°21′ N to 30°01′ N and longitude 106°56′ E to 107°43′ E, the total area is 2941.46 km^2 (Guan et al. 2018). The Hydro-fluctuation Belt of Three Gorges Reservoir can adjust the water level fluctuation to meet the needs of power generation and Flood Control in Hydraulic Engineering. Its water surface area between the highest water level line in flood period and the lowest water level in dry season of reservoir has the obvious plant community gradient, environmental impact factor and ecological process characteristic. Therefore, this region has high ecological vulnerability and is easy to be polluted and damaged.

2.2 Data processing

2.2.1 Extracting the fluctuating zone in Fuling district

The eigenvalue method as a new method of water body information extraction is proposed. Band 5 in RS image has best effect to distinguish roads, soil and water. Although band 3 can also be a good monitoring of the road and the soil, it has poor ability to identify water. So, water information can be well identified through removal of road and soil from three objects which are identified in band 5. This method is more efficient, simple and rapid than the commonly used methods such as Multi band spectral correlation method, Normalized Difference Water Index (NDWI) and Modified Normalized Differences Water Index (MNDWI), and the extraction of water body boundary with this method is much clearer. Using eigenvalue method to extract the water image from highest water level (175m in October 31, 2010) and the lowest water level (145m in August 25, 2010) at the same period. And difference vector image between the highest water level and the lowest water level is calculated in ArcGIS. The Three Gorges Reservoir's vector map is cut with Fuling area vector data to obtain the Fuling section hydro-Fluctuation Belt in the Three Gorges Reservoir (**Fig.1**), the total area is 20.49 km^2 (Guan et al., 2018).

2.2.2 Estimation of vegetation coverage of reservoir

A linear mixed spectral model is used to estimate the vegetation coverage of the Fuling section of the Three Gorges Reservoir area (Li et al. 2015).

Firstly, Pixel Purity Index algorithm which is semi-automatic end member extraction method is employed to extract the end-element of image under the guidance of prior knowledge. The extraction using the PPI algorithm is based on the linear mixing spectral models and the principle that end-element is endpoint of convex simplex formed by remote sensing image in feature space (Rahmati and Hamzehpour 2017). The process can be divided into three steps:

The first step is Minimum Noise Fraction Transform (MNF). According to the correlation between each band, band 1, band 2, band 3, band 4, band 5 and band 7 of image are integrated for minimum noise separation. The results are shown in **Fig.2**.

The second step is the calculation of Pixel Purity Index. In this study, a certain threshold is set to obtain end-element colony in region of interest (ROI) from PPI image. The number of iterations is 10000 times, and the iterative factor is 2.5. The pixel in the ROI is a pure pixel, which is used for the selection of the end-element and spectra in the N dimensional visualization analysis, as shown in **Fig. 3**.

The third step is N dimensional visualization analysis. The purpose of the N dimensional visual analysis tool for human-computer interaction is to determine the end-element of image. Clicking on four components in the window can build a scatter plot. Then, the image spatial

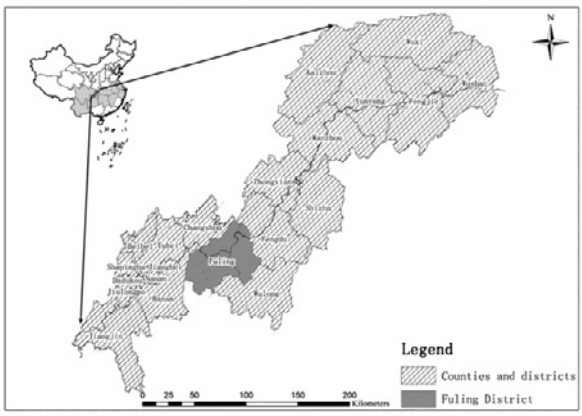

Fig. 1. A map of study area.

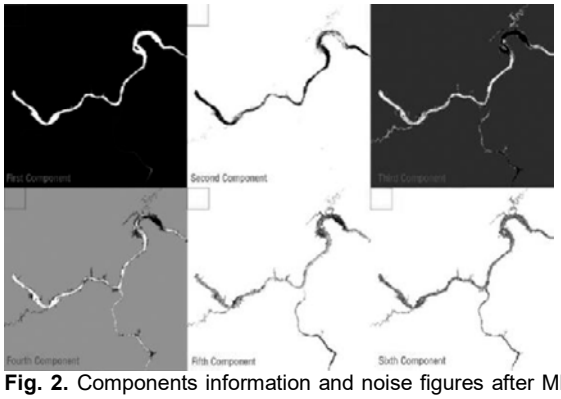

Fig. 2. Components information and noise figures after MNF transformation.

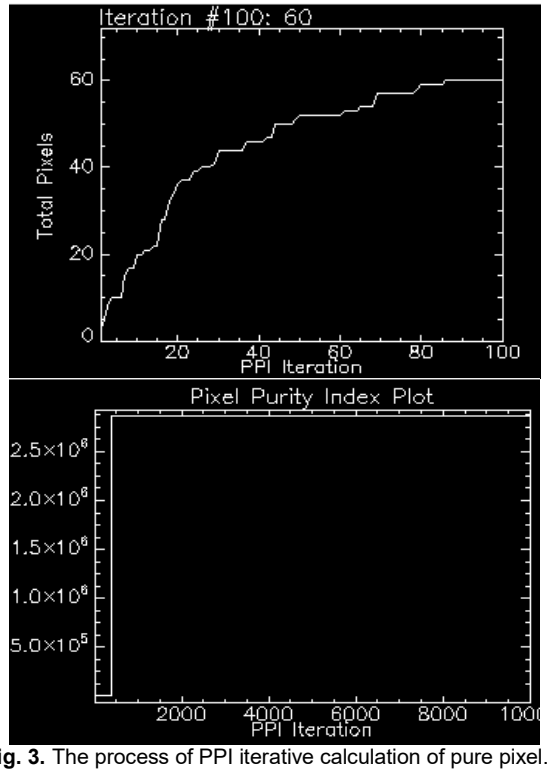

Fig. 3. The process of PPI iterative calculation of pure pixel. Progress：Left is 1%, Right is 100%.

feature should be combined with spectral feature of a prior ground object. Subsequently, different colors are selected to indicate and select the data points at the corner or the relatively independent data points in the four-dimensional dynamic image. And, partial regions around the scatter plot need be highlighted. Afterwards, average spectra from original image of study area is selected as the end-element spectrum to determine the type of end-element and spectral information, as shown in **Fig.4**. As can be seen from the spectral characteristic curve in **Fig.5**, four types of end-elements reflect the obvious spectral characteristics of different objects, and in the third wave band, the vegetation spectrum appears steep slope to reach a peak value.

Secondly, this research uses the linear spectral tools to solve the linear spectral decomposition model with unconstrained condition, the general formula is as follows:

$$p = \sum_{i=1}^{N} c_i e_i + n = Ec + n \quad [1]$$

Where: E is the end-element vector; c is abundance values of various types of ground objects; n is error term.

The result of linear spectral decomposition model with unconstrained condition is shown below.

Finally, the terminal unit spectra used in the SAM model come from ASCII files of all types of end-element spectra obtained after the end-element extraction. If the angle is small, it represents the close match with the reference spectra; if the angle is large, it indicates that the pixel is far away from the specified radian threshold and cannot be classified. The classification formula is as follows:

$$S = \cos^{-1}\left(\sum_{i=1}^{n} t_i r_i \Big/ \sum_{i=1}^{n} \left(t_i^2\right)^{1/2} \sum_{i=1}^{n} \left(t_i^2\right)^{1/2} \right) \quad [2]$$

Where: t_i is spectrum of ground object to be classified; r_i is the spectrum of the reference end element after extracted; n is band number.

After calculating the classification, error and leakage pixel objects need be manually divided into various categories according to false color composite image of wave band 432.

The spectral angle classification results of the five images are verified by Kappa coefficient accuracy. The evaluation results of image classification accuracy are shown in the following **Table 1 to Table 5**.

It can be seen from **Table 1 to Table 5**, using the spectral angle classification model can make overall accuracy of average classification. The overall accuracy

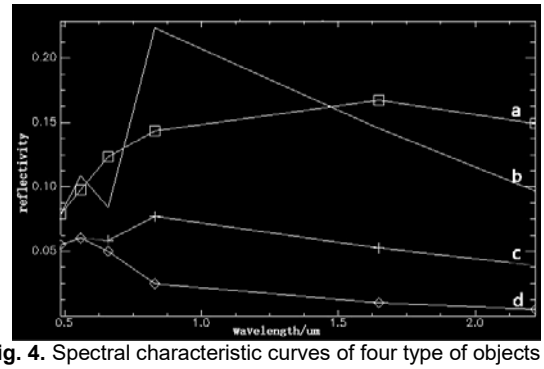

Fig. 4. Spectral characteristic curves of four type of objects a) Bare soil; b) Terrestrial plant; c) Hygrophytes; d) Water

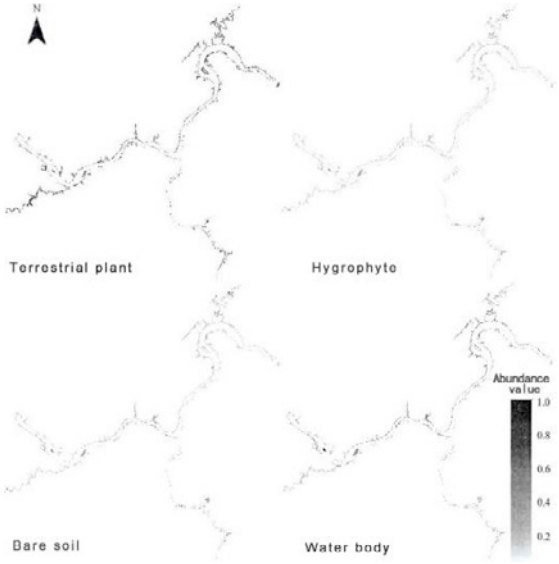

Fig. 5. The distribution maps of abundance values of four type ground objects solved by Hybrid spectral model.

Table 1. Classification accuracy parameters in 2003.

Ground object type	Terrestrial plant	Hygrophyte	Bare soil	Water body
Terrestrial plant	63	0	0	0
Hygrophyte	1	45	6	0
Bare soil	0	0	32	0
Water body	0	0	0	42
Drawing accuracy/%	98.44	100.00	84.21	100.00
User accuracy/%	100.00	86.54	100.00	100.00
Overall accuracy/%	96.16			
Kappa coefficient	0.9486			

in 2003, 2004, 2008, 2010 and 2018 reach to 96.16%, 94.69%, 96.55%, 89.86% and 94.11, respectively. And the average Kappa coefficient in 2003, 2004, 2008, 2010 and 2018 reach to 0.9486, 0.9213, 0.9532, 0.8816, and 0.9247, respectively. It is evident that the spectral angle classification is reliable for assessing vegetation coverage type of Fuling Hydro-Fluctuation Belt in the Three Gorges Reservoir Area.

3. Results and discussion

3.1 Analysis of the dynamic degree of the ground object type in the reservoir fluctuating zone

The area value of each wetland land use types in the spatial distribution pattern map of wetland vegetation of the five periods in Fuling section Hydro-fluctuation belt of the Three Gorges Reservoir were statistically. The results are shown in the following **Fig.6**.

Single dynamic degree analysis can be used to analyze the variation of land use types in the fluctuating zone in a certain time range. It can be seen from the **Fig. 7** that the fastest annual change of land use type is hygrophyte from 2003 year to 2004 year, and the annual change rate is 107.75%; followed by bare soil, the annual change rate is 62.37%; from 2004 to 2008, the fastest annual change is the bare soil, the growth rate is 61.84%, the slowest annual change is the vegetation, the average change rate only around 5%; bare soil showed a decreasing trend in 2008-2010, the reduction rate was 51.1%; from 2010-2013 ,the change rate of wetland utilization types was small in, showing a gradually stable trend. During 10 years from 2003 to 2013, the fastest growth was the hygrophyte with a comprehensive growth rate of 113.71%, followed by bare soil, the growth rate was 100.75%, the land plants and water body were reduced, and the reduction rate was 24.66% and 30.87%, respectively.

Comprehensive dynamic degree can be used to analyze the speed of land use change. It can be seen from the **Fig.8** that the comprehensive variation of terrestrial and hygrophyte showed a small fluctuation trend, indicating that the changes of terrestrial and hygrophyte showed a stable trend, and that the water body showed a moderate fluctuation trend, and the trend of the three land types showed a tendency appear increase-decrease-increase-decrease. it is indicated that the changes of terrestrial and hygrophyte are closely related to the water body. And the comprehensive change of the bare soil is the most intense. It can be seen that the trend of drastic reduction of bare soil is closely related to the factors of human disturbance. Overall, the comprehensive dynamic degree of land use types is decrease in the fluctuation zone, indicating that the stability of the fluctuation zone is gradually increasing.

3.2 Spatial distribution prediction of vegetation in hydro-fluctuation belt

This paper uses CA-Markov model for the neighbor relation analysis which not only contributes to accurate

Table 2. Classification accuracy parameters in 2004.

Ground object type	Terrestrial plant	Hygrophyte	Bare soil	Water body
Terrestrial plant	87	0	0	0
Hygrophyte	0	74	0	0
Bare soil	0	0	36	0
Water body	0	13	0	35
Drawing accuracy/%	100.00	85.06	100.00	100.00
User accuracy/%	100.00	100.00	100.00	72.92
Overall accuracy/%	94.69			
Kappa coefficient	0.9213			

Table 3. Classification accuracy parameters in 2008.

Ground object type	Terrestrial plant	Hygrophyte	Bare soil	Water body
Terrestrial plant	75	0	0	0
Hygrophyte	4	80	0	0
Bare soil	6	0	67	0
Water body	0	0	0	50
Drawing accuracy/%	88.24	100.00	100.00	100.00
User accuracy/%	100.00	95.24	91.78	100.00
Overall accuracy/%	96.55			
Kappa coefficient	0.9532			

Table 4. Classification accuracy parameters in 2010.

Ground object type	Terrestrial plant	Hygrophyte	Bare soil	Water body
Terrestrial plant	60	0	0	0
Hygrophyte	9	88	5	0
Bare soil	4	0	48	0
Water body	0	0	10	52
Drawing accuracy/%	82.50	100.00	76.19	100.00
User accuracy/%	100.00	86.25	92.31	84.17
Overall accuracy/%	89.86			
Kappa coefficient	0.8816			

Table 5. Classification accuracy parameters in 2013.

Ground object type	Terrestrial plant	Hygrophyte	Bare soil	Water body
Terrestrial plant	75	2	0	0
Hygrophyte	1	30	0	5
Bare soil	0	5	50	0
Water body	0	2	0	85
Drawing accuracy/%	98.68	76.19	100.00	94.45
User accuracy/%	97.40	84.12	90.91	97.70
Overall accuracy/%	94.11			
Kappa coefficient	0.9247			

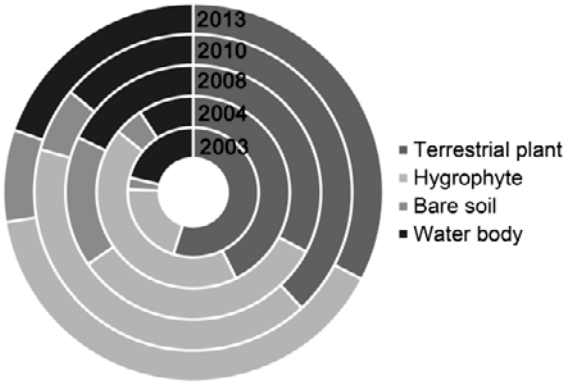

Fig. 6. Areas of land use types from 2003 to 2013.

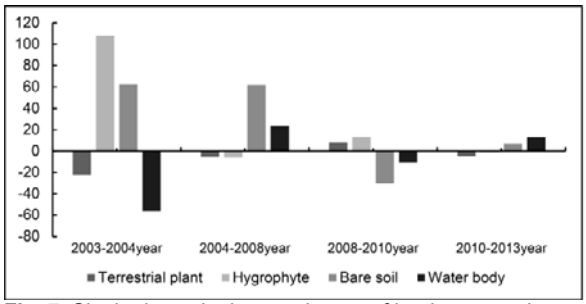

Fig. 7. Single dynamic degree change of land use type in fluctuating belt at different times.

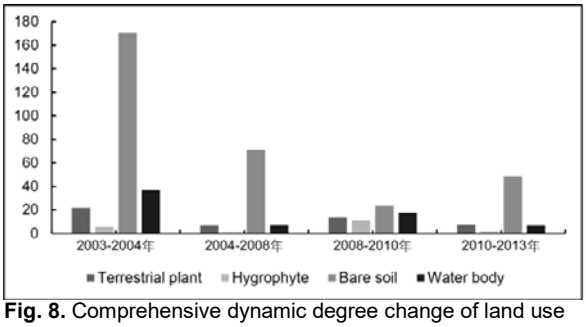

Fig. 8. Comprehensive dynamic degree change of land use type in fluctuating belt at different times.

predict the future land use quantity structure based on the Markov chain, but also strengthens the simulation ability of spatial pattern.

According to wetland utilization type of hydro-fluctuation belt in 2008 year and 2013 year, the state transition matrix of each year is predicted, as shown in the **Table 6-9**.

As predicted in the above tables, during five years from 2013 to 2018, the terrestrial plant will decrease 0.5871 km^2, hygrophyte will increase 0.1795 km^2, bare soil will decrease 0.1026 km^2 and water will be increased 0.5102 km^2. Furthermore, during ten years from 2013 to 2023, terrestrial plant will decrease 0.7432 km^2, hygrophyte will decrease 0.0114 km^2, bare soil will decrease 0.1155 km^2 and water will increase 0.8703km^2. During fifteen years from 2013 to 2028, terrestrial plant will decrease 0.7877 km^2, hygrophyte will decrease 0.0843 km^2, bare soil will decrease 0.1417 km^2 and water will increase 1.0136km^2. During twenty years from 2013 to 2033, terrestrial plant will decrease 0.8023 km^2,

Table 6. Transition probability matrix of land use type in hydro-fluctuation belt from 2013 to 2018.

		2018 year			
		Terrestrial plant	Hygrophyte	Bare soil	Water body
2013 year	Terrestrial plant	0.3431	0.4555	0.0838	0.1175
	Hygrophyte	0.2445	0.4219	0.0807	0.2530
	Bare soil	0.5458	0.2890	0.1467	0.0184
	Water body	0.2292	0.3449	0.0157	0.4102

Table 7. Transition probability matrix of land use type in hydro-fluctuation belt from 2013 to 2023.

		2023 year			
		Terrestrial plant	Hygrophyte	Bare soil	Water body
2013 year	Terrestrial plant	0.2346	0.4742	0.0828	0.2083
	Hygrophyte	0.3229	0.3156	0.0783	0.2833
	Bare soil	0.3774	0.4219	0.0675	0.1332
	Water body	0.2795	0.4286	0.0510	0.2409

Table 8. Transition probability matrix of land use type in hydro-fluctuation belt from 2013 to 2028.

		2028 year			
		Terrestrial plant	Hygrophyte	Bare soil	Water body
2013 year	Terrestrial plant	0.2205	0.4616	0.0763	0.2416
	Hygrophyte	0.3330	0.3097	0.0766	0.2807
	Bare soil	0.3164	0.4296	0.0557	0.1983
	Water body	0.2960	0.4403	0.0635	0.2002

Table 9. Transition probability matrix of land use type in hydro-fluctuation belt from 2013 to 2033.

		2033 year			
		Terrestrial plant	Hygrophyte	Bare soil	Water body
2013 year	Terrestrial plant	0.2162	0.4566	0.0735	0.2537
	Hygrophyte	0.3348	0.3094	0.0765	0.2793
	Bare soil	0.2987	0.4246	0.0515	0.2251
	Water body	0.3030	0.4433	0.0679	0.1858

hygrophyte will decrease 0.1162km^2, bare soil will decrease 0.1504 km^2 and water will increase 1.0687km^2. The increase of water area and hygrophyte area indicate that frequently water flooded has great influence on the growth and evolution of plants, and the long-term water flooded of the terrestrial plants will be gradually transformed into hygrophytes.

Based on the data of 2013 year, we are predict the wetland utilization type of Fuling section hydro-Fluctuation Belt in the Three Gorges Reservoir in 2018，2023，2028 and 2023 year. The main change trend of terrestrial plants is decreasing yearly and the decrement is also decreasing yearly. The wetland plant is increasing in 2018 year and then will decrease yearly. The bare soil remains basically unchanged with maintaining a relatively stable level. The water coverage is increasing yearly and has the largest increase amplitude as compared with

other types. To a certain extent, it can be concluded that the stability of the hydro-fluctuation belt slope is low and affected greatly by the water body function. Further research is needed. Therefore, the CA-Markov model is used to compute probability matrix and then forecast the wetland utilization type layout for various years of hydro-fluctuation belt. As shown in **Fig.9**. The results showed that the terrestrial plants and water body will continue to decrease, hygrophyte will continue to increase, the bare soil is relatively stable.

4. Conclusions

This study analyzed the dynamic changes of wetland use types in Fuling area Hydro-fluctuation belt from the aspects of area change and structure change based on the evolution rule of past vegetation type. The Markov model was used to calculate the probability transfer matrix of the wetland utilization types in each period, and the CA-Markov model was used to simulate the distribution patterns of wetland utilization patterns in the future. It is found that high coverage area of terrestrial plant is mainly distributed in the tributary of the northeast and southwest of the study area; hygrophyte is characteristics of linear distribution along the waterfront; bare soil mainly shows the scattered distribution in other areas. Meanwhile, spectral angle classification for five images is performed according to the spectral reflectance curve of the end-element. The classification results have a high accuracy, illustrating that classification effect is relatively rational. Our results can provide a reference support for restoration and development planning scheme of the hydro-fluctuation belt in the Three Gorges Reservoir.

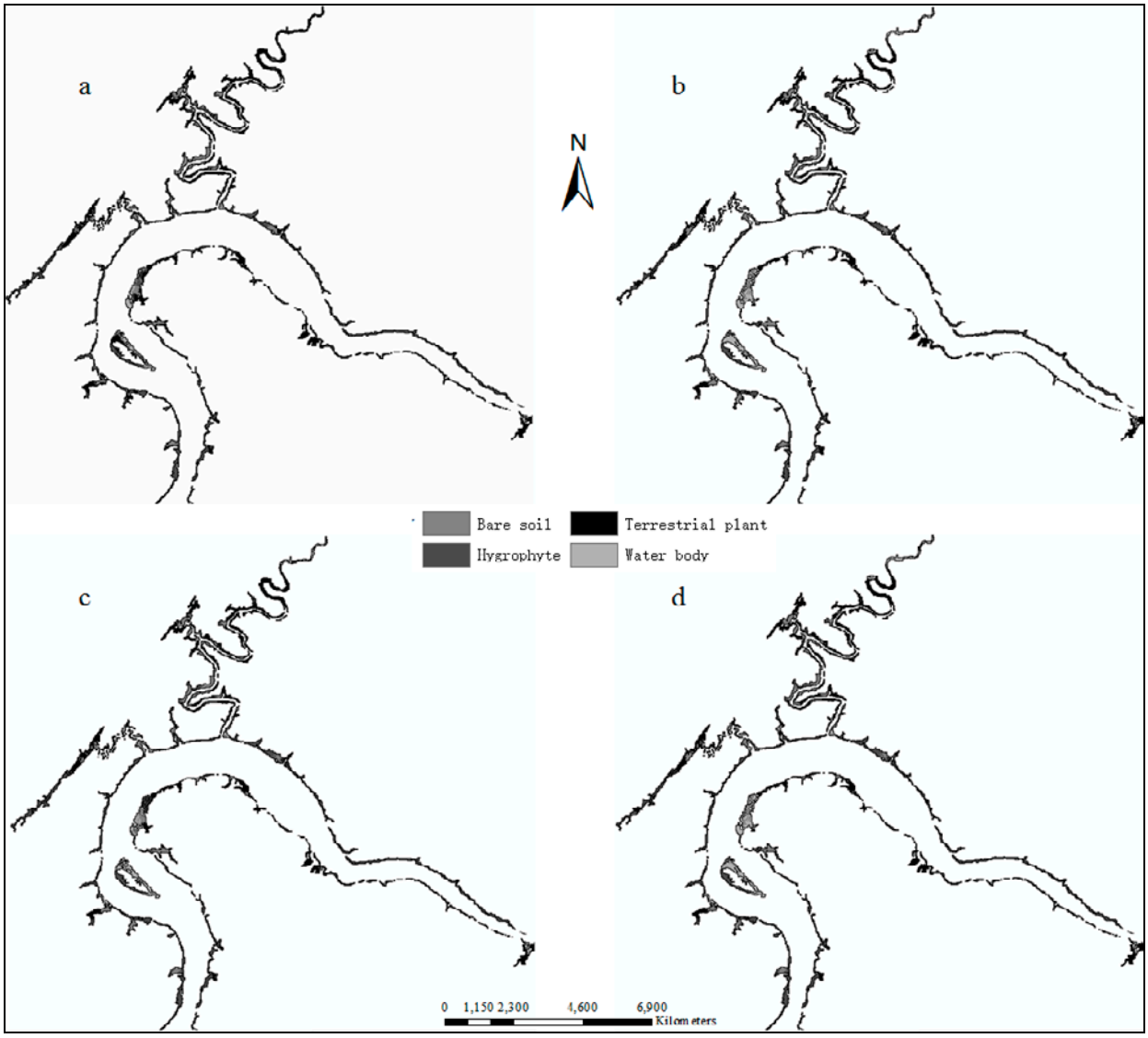

Fig. 9. Vegetation distribution prediction map of hydro-fluctuation belt from 2018 to 2033 (Section)

Note: a, b, c and d present simulation results of 2018, 2023, 2028 and 2033, respectively.

Acknowledgments

This work is partially supported by the Science and Technology Research Program of Chongqing Municipal Education Commission (No.KJZD-K201800702), Basic Science and Advanced Technology Fund of Chongqing Scientific Council in China (No. cstc2017jcyjAX0210) and Fund of Key Laboratory of New Technology for Construction of Cities in Mountain Area of Chongqing University in China (No. 0902071812102/012).

Reference

Gao, XH. Xiang, LB. Wei, RY., 2011. Research on the algorithm of end element extraction based on spectral classification. Spectroscopy and Spectral Analysis, 2011, **31** (7):1995-1998.

Guan, DJ., Qu, SJ., Yang, SS. and He, XJ., 2018, Spatio-Temporal Evolution Process of Vegetation Coverage of Hydro-Fluctuation Belt in Three Gorges Reservoir Based on GIS-RS. Journal of Chongqing Jiaotong University(Natural Science), **37** (6).(in Chinese)

Guan, DJ ., Li, HF., Inohae, T., Su, WC., Nagaie, T. and Hokao, K., 2011.Modeling urban land use change by the integration of cellular automaton and Markov model. Ecological Modelling, **222** (20-22): 3761-3772.

Huang, XH., Liu, Y., Li, JX., Xiong, XZ., Chen, YH., Yin, XH. and Feng, DL., 2013. The response of mulberry trees after seedling hardening to summer drought in the hydro-fluctuation belt of Three Gorges Reservoir Areas. Environmental Science and Pollution Research, **20** (10): 7103-7111.

Jiang, P., Shi, DM., Hu, XQ., Huang, XZ., Li, YX. And Guo, TL., 2015. Soil stability characteristics of mulberry lands at hydro-fluctuation belt in the Three Gorges Reservoir area, China. Environmental Monitoring and Assessment, **187** (10). https://doi.org/10.1007/s10661-015-4834-6

Li, HY., Zhou, PJ., Xu, C., Zhang, WS. and Song, GQ., 2016. Research on Vegetation Ecological Risk Assessment Based on Rrm-Take Xiangxi River Hydro-Fluctuation Belt of Three Gorges Reservoir Area as an Example. Fresenius Environmental Bulletin, **25** (2): 419-428.

Li, Y., Wang, H. and Li, XB., 2015. Fractional Vegetation Cover Estimation Based on an Improved Selective Endmember Spectral Mixture Model. PLoS One, **10** (4). https://doi.org/10.1371/journal.pone.0124608

Li., ZL., Hasi, B. and Yoshiki, Y., 2018. Analysis of spatiotemporal land cover changes in Inner Mongolia using self-organizing map neural network and grid cells method. Science of the Total Environment, 636:1180-1191.

Lin, WP., Cen, JW., Xu, D., Du, SQ. and Gao, J., 2018. Wetland landscape pattern changes over a period of rapid development (1985-2015) in the ZhouShan Islands of Zhejiang province, China. Estuarine Coastal and Shelf Science, **213**:148-159.

Liu, Y. and Willison, JHM., 2013. Prospects for cultivating white mulberry (Morus alba) in the drawdown zone of the Three Gorges Reservoir, China. Environmental Science and Pollution Research, **20** (10):7142-7151.

Liu, Y., Willison, JHM., Wan, P., Xiong, XZ., Ou, Y., Huang, XH., Wu, JC., Zhou, H., Xu, Q., Chen, GH., Xili, YZ. and Nie, JS., 2016. Mulberry trees conserved soil and protected water quality in the riparian zone of the Three Gorges Reservoir, China. Environmental Science and Pollution Research, **23** (6): 5288-5295.

Liu, T., Amr, AE., Alina, Z., ; Zare, A., Dewitt, BA., Flory, L. and Smith, SE., 2018. A fully learnable context-driven object-based model for mapping land cover using multi-view data from unmanned aircraft systems. Remote Sensing of Environment, **216**: 328-344.

Ma, WC., Wei, H., Liu, Y., Wang, T., Zhou, C., Wang, ZX. and Zhang, YY., 2016. Effect of Water Flooding and Planting Density on the Chlorophyll Fluorescence Response in Cocultivated Cynodon Dactylon and Hemarthria Altissima. Fresenius Environmental Bulletin, **25** (12): 5599-5610.

Mariana, T., Liliana, P. and Roberto, MH., 2019. Hybrid spatiotemporal simulation of future changes in open wetlands: A study of the Abitibi-Temiscamingue region, Quebec, Canada. International Journal of Applied Earth Observation and Geoinformation, 74:302-313.

Nie, YD., Zhang, Z., Wang, M., Shen, Q., Li, YF., Gao, WJ. and Yang, L., 2017. Seasonal variations of carbonic anhydrase activity in Chongqing urban section of Jialing River and its influencing factors. Chemosphere, **179**: 202-212.

Rahmati, M. and Hamzehpour, N., 2017. Quantitative remote sensing of soil electrical conductivity using ETM plus and ground measured data. International Journal of Remote Sensing , **38** (1): 123-140.

Wan, LP., Zhou, ML. and Desar, S., 2017. Long-Term Stability Calculation of Reservoir Bank Slope Considering Water-Rock Interaction. Tehnicki Vjesnik, **24** (1): 283-289.

Zhang, ZM., Ouyang, ZY., Xiao, Y., Xiao, Y. and Xu, WH., 2017. Using principal component analysis and annual seasonal trend analysis to assess karst rocky desertification in southwestern China. Environmental Monitoring and Assessment, **189** (6). https://doi: 10.1007/s10661-017-5976-5.